An Optimal Basis of Band-Limited Functions for Signal Analysis and Design

Liying Wei, *Student Member, IEEE*, Rodney A. Kennedy, *Fellow, IEEE*, and Tharaka A. Lamahewa, *Member, IEEE*

***Abstract*—This paper studies signal concentration in the time and frequency domains using the general constrained variational method of Franks. The minimum kth $(k = 0, 2, 4, \ldots)$ moment time-duration measure for band-limited signals is formulated. A complete, orthonormal set of band-limited functions in $L^2([-W, W])$ with the minimum fourth-moment time-duration measure is obtained. Numerical investigations of our optimal 4th moment functions show: 1) less energy concentration in the main lobe than the prolate spheroidal wave functions (PSWF); 2) higher energy concentration in the main lobe than Gabor's function; and 3) a larger main lobe than both PSWF and Gabor. Applications for our basis functions include: 1) radar systems and high resolution communication systems, and 2) representation and approximation to any band-limited signal in a given time interval.**

***Index Terms*—Fraction out-of-band energy (FOBE), Gabor's function, orthonormal basis, prolate spheroidal wave function (PSWF), time-frequency.**

I. Introduction

It is well known that a signal with shorter pulse duration has better range resolution [1] and a signal with smaller bandwidth better utilizes scarce channel frequency resources. But according to the Fourier transform theory, a signal cannot be both time-limited and band-limited simultaneously. However, in tasks such as minimizing the error rate [2]–[4] or minimizing bias for high-resolution spectral estimation [5], researchers seek signal designs that have the greatest concentration simultaneously in both time and frequency domains [6].

Slepian and Pollak [3] developed a set of concentration results which are particularly relevant to practical applications. For a band-limited signal which is confined to the frequency range $[-W, W]$, the fraction out-of-band energy (FOBE) measure was proposed to determine a signal that has the greatest portion of its energy in the $[-T, T]$ time interval. These signals are the prolate spheroidal wave functions (PSWF). There are similar results when we exchange the roles of the time and frequency domains.

Further interest in concentration for time-limited signals saw the emergence of other results, such as minimum bandwidth of M orthogonal signals [7] and minimum root-mean-square (RMS) bandwidth of M time-limited signals [8]. Similarly, band-limited signals with minimum time-duration also have wide applicability, such as hearing sensation [9], extrapolation of band-limited signals [10], [11], optimal waveform signal design [12] and resolution enhancement to the near-field acoustic holography [13].

Slepian [14] also extended his results to the discrete case. The corresponding optimal functions are called the discrete prolate spheroidal wave functions (DPSWF). Applications of this result include digital filter design [15], optimal windows design in electroencephalogram (EEG) [16], reduction of the bias of multitaper spectrum estimation in geophysics [17], and local basis expansions for linear inverse problems [18]. Recently, the DPSWF functions have also been applied in constructing wavelets for multi-resolution analysis [19]–[22], and shown potential in denoising for image processing.

However, no explicit analytical formula for prolate spheroidal wave function (PSWF) has been developed. In addition, the cost in calculating such a solution to a second-order differential operator which commutes with the PSWF integral convolution operator [3] is expensive [23]. At present, only the discrete version of PSWF is available [3], [24]–[26]. The PSWF decays slowly like $1/t$ for increasing time t. In contrast, Gabor's optimal band-limited function, i.e., the half sinusoid signal, which minimizes a second-moment concentration measure, decays more quickly as $1/t^2$. In [27], an optimal time-limited function with the minimum fourth-moment bandwidth was determined. This function has larger main lobe and decays as $1/f^3$. However, a detailed formulation and analysis for band-limited signals and their concentration properties with arbitrary moment weighting in the time-domain is of interest here. Furthermore, we also investigate whether alternative complete, orthonormal set of band-limited functions, besides PSWFs, exists which have better performances than the PSWF in representing a band-limited function and approximating a band-limited function.

In this paper, we apply the *general constrained variational method* of Franks [28] to formulate concentration with a kth time moment weighting for a band-limited signal. The case $k = 4$ is taken as a central example. A complete, orthonormal set of optimal band-limited functions in $L^2([-W, W])$ with the minimum fourth-moment time-duration measure is obtained. The characteristics of the set of functions are discussed. Further, the minimum fourth-moment time-duration measure and the time-duration energy concentration measure are calculated. Furthermore, by comparing the PSWF and Gabor's functions, our optimal functions can be a seen to be a good alternative in optimal

Manuscript received December 23, 2009; accepted June 19, 2010. Date of publication July 12, 2010; date of current version October 13, 2010. The associate editor coordinating the review of this manuscript and approving it for publication was Dr. Maja Bystrom. This work was supported by the Australian Research Council Discovery Grant DP1094350.

The authors are with the Research School of Information Sciences and Engineering, School of Engineering, College of Engineering and Computer Science, The Australian National University, Canberra, ACT 0200, Australia (e-mail: liying.wei@rsise.anu.edu.au; rodney.kennedy@anu.edu.au; tharaka.lamahewa@anu.edu.au).

Digital Object Identifier 10.1109/TSP.2010.2057427

waveform design for communication systems, and higher range resolution radar systems. Finally, this set of optimal functions can also be used for representation of any band-limited signal, extrapolation a band-limited function known only in the interval $[-T,T]$ or approximation a band-limited function in the interval $[-T,T]$.

The rest of the paper is organized as follows. We present the problem in Section II. Section III presents the general constrained variational method of Franks [28]. In Section IV, the minimum fourth-moment time-duration concentration measure problem is formulated, and then a complete, orthonormal set of optimal band-limited functions is obtained. Further, the properties of this set of functions are studied in Section V. Section VI gives two practical applications for the set of functions. Finally, we conclude the paper in Section VII.

II. Problem Formulation

Let L^2 be the complex Hilbert space containing all square-integrable functions defined on the real line with inner product defined as

$$\langle x,y\rangle = \int_{-\infty}^{\infty} x(t)\overline{y(t)}\,dt.$$

for $x,y \in L^2$. This inner product induces the norm such that $\|x\| = \langle x,x\rangle^{1/2}$.

Find the optimal finite energy signal, $x(t) \in L^2$, band-limited to the frequency range $[-W,W]$ which minimizes the moment weighted energy $\int_{-\infty}^{\infty} t^k|x(t)|^2\,dt$. Here t^k, $k=0,2,4,\ldots$, is the kth weighting function in the time-domain. Note that odd values of k and $k=0$ are degenerate or trivial. For $k=2$, this problem has been solved by Gabor [9]. In this paper, we concentrate on the $k=4$, fourth moment time-domain weighting as an exemplar. For $k>4$, the solution can be easily extended based on our methods. It is possible to treat the case of time-limited finite energy signals with frequency domain moment weighting f^k in an analogous way.

III. General Constrained Variational Method

In this section, we first revisit the general constrained variational method of Franks [28, Ch. 6]. This method is applicable for any properly formulated extremization problem in the time and frequency domains, and is ideal for signal concentration problems.

The general constrained variational problem is stated: For a given signal with finite energy, extremize (maximize or minimize) the arbitrary weighted energy either in the time-domain or in the frequency domain, to obtain the optimal waveform signal. Suppose $w(t) \geq 0$ is an arbitrary weighting function in the time-domain, $V(f) \geq 0$ is an arbitrary weighting function in the frequency domain. Following Franks [28], this general variational problem is equivalent to extremizing

$$G = \mu_1 I_1 + \mu_2 I_2 + I_3 \tag{1}$$

where μ_1 and μ_2 are two Lagrange multipliers and I_1, I_2 and I_3 are three quadratic functionals defined as

$$I_1 \triangleq \langle wx,x\rangle = \int_{-\infty}^{\infty} w(t)|x(t)|^2\,dt$$
$$I_2 \triangleq \langle VX,X\rangle = \int_{-\infty}^{\infty} V(f)|X(f)|^2\,df$$
$$I_3 \triangleq \langle x,x\rangle = \langle X,X\rangle = 1.$$

Here, I_1 represents a time weighted measure of energy in the time domain, I_2 represents a frequency weighted measure of energy in the frequency domain, and I_3 represents the total energy of a signal constrained to be unity (finite energy without loss of generality). The frequency domain inner product is defined in the obvious way.

By solving this optimization (1), the necessary conditions are obtained both in time-domain and frequency domain [28]

$$\mu_1 w(t)x(t) + \mu_2 \int_{-\infty}^{\infty} v(t-\tau)x(\tau)d\tau + x(t) = 0$$
$$\mu_1 \int_{-\infty}^{\infty} W(f-\nu)X(\nu)d\nu + \mu_2 V(f)X(f) + X(f) = 0 \tag{3}$$

where $v(t)$ is the inverse Fourier transforms of $V(f)$ and $W(f)$ is the Fourier transform of $w(t)$.

IV. Fourth-Moment Time-Duration Concentration Measure

In this section, using the Franks' general constrained variational method, we formulate the fourth-moment time-duration concentration measure to a band-limited signal with maximum bandwidth W. The optimal band-limited signals with the minimum fourth-moment time-duration concentration measure are obtained. These optimal functions consist of a complete, orthonormal basis for $L^2([-W,W])$ which is the Hilbert space of band-limited functions with maximum bandwidth W (which can be regarded as a subspace of L^2). The comparison between these functions and Gabor's band-limited functions which have the second-moment weighting in the time-domain is made. Some of these results have been presented in [29].

A. Optimization Formulation

Define frequency weighting, corresponding to band-limiting to frequencies $[-W,W]$

$$V(f) = \begin{cases} 1, & |f| \leq W \\ 0, & |f| > W \end{cases} \tag{4}$$

and time weighting

$$w(t) = t^4,$$

corresponding to fourth moment time-domain weighting. Then under the general constrained variational method of Franks, the optimization problem is to extremize

$$G(x) = \mu_1 I_1 + \mu_2 I_2 + I_3$$

where

$$I_1 = \int_{-\infty}^{\infty} t^4 |x(t)|^2 dt$$
$$I_2 = \int_{-\infty}^{\infty} V(f)|X(f)|^2 df = \int_{-W}^{W} |X(f)|^2 df = 1$$
$$I_3 = \langle x, x\rangle = \langle X, X\rangle = 1.$$

Now to obtain the optimal function $X(f)$ that renders $G(x)$ or I_1 stationary, we only need to find the necessary condition in the frequency domain.

Using the Fourier transform of $t^n f(t)$

$$t^n f(t) \longleftrightarrow i^n \frac{d^n F(\omega)}{d\omega^n} = \frac{i^n}{(2\pi)^n} \frac{d^n F(f)}{df^n}$$

where $i = \sqrt{-1}$, the necessary condition (3) in the frequency domain is obtained

$$\mu_1 \frac{1}{(2\pi)^4} X^{(4)}(f) + \mu_2 V(f) X(f) + X(f) = 0, \quad |f| \le W$$

which further simplifies to the fourth-order linear differential equation

$$X^{(4)}(f) = -\frac{1+\mu_2}{\mu_1}(2\pi)^4 X(f), \quad |f| \le W \tag{6}$$

where the notation $X^{(4)}(f)$ represents the fourth derivative of $X(f)$ with respect to frequency f. By defining $\lambda = -(1+\mu_2)(2\pi)^4/\mu_1 \in \mathbb{R}$ (real numbers), this equation can be written

$$(D^4 X)(f) = \lambda X(f), \quad |f| \le W \tag{7}$$

where D is the differential operator. Revealing this is an eigenfunction equation with λ the eigenvalue.

B. Solutions

A general solution to the fourth-order linear differential equation (7) can be written as

$$X(f) = A\cos(mf) + B\sin(mf) + E\cosh(mf) + F\sinh(mf), \quad |f| \le W$$

where A, B, E, and F are arbitrary constants. Its first derivative is

$$X'(f) = m(-A\sin(mf) + B\cos(mf) + E\sinh(mf) + F\cosh(mf)), \quad |f| \le W.$$

According to the characteristics of $X(f)$, specifically: the boundary conditions $X(-W) = X(W) = 0$ and $X'(-W) = X'(W) = 0$, and the total energy of $I_3 = \langle x, x\rangle = \langle X, X\rangle = 1$, there are three different solutions.

Case a): When $X(f)$ is an even function, i.e., $B = F = 0$, then

$$X_e(f) = A_e(\cos(mf) + \alpha\cosh(mf)), \quad |f| \le W \tag{9}$$

where $A_e = 1/\sqrt{(1+\alpha^2)W}$, $\alpha = -\cos(mW)/\cosh(mW)$ and m is a positive solution of the following even condition equation:

$$C_e(m) \triangleq \cos(mW)\sinh(mW) + \sin(mW)\cosh(mW) = 0. \tag{10}$$

Case b): When $X(f)$ is an odd function, i.e., $A = E = 0$, then

$$X_o(f) = B_o(\sin(mf) + \beta\sinh(mf)), \quad |f| \le W \tag{11}$$

where $B_o = 1/\sqrt{(1-\beta^2)W}$, $\beta = -\sin(mW)/\sinh(mW)$ and m is a positive solution of the following odd condition equation:

$$C_o(m) \triangleq \cos(mW)\sinh(mW) - \sin(mW)\cosh(mW) = 0. \tag{12}$$

Case c): When $X(f)$ is neither an even nor an odd function, it can be expressed as a linear combination of (9) and (11). Note the values of m in (9) and (11) are not the same.

C. Inverse Fourier Transform

Taking the inverse Fourier transform of $X(f)$, we find the optimal signal waveform $x(t)$ in the time-domain.

For $|f| \le W$, we have the following Fourier transform pairs:

$$\frac{W}{2\pi}\left\{\mathrm{sinc}\left[W\left(t+\frac{m}{2\pi}\right)\right] + \mathrm{sinc}\left[W\left(t-\frac{m}{2\pi}\right)\right]\right\} \longleftrightarrow \cos(mf)V(f)$$

and

$$-\frac{iW}{2\pi}\left\{\mathrm{sinc}\left[W\left(t+\frac{m}{2\pi}\right)\right] - \mathrm{sinc}\left[W\left(t-\frac{m}{2\pi}\right)\right]\right\} \longleftrightarrow \sin(mf)V(f)$$

where $\mathrm{sinc}(x) = \sin x/x$ and $V(f)$ is defined in (4).

Similarly, we have

$$\frac{W}{2\pi}\left\{\mathrm{sinc}\left[W\left(t+i\frac{m}{2\pi}\right)\right] + \mathrm{sinc}\left[W\left(t-i\frac{m}{2\pi}\right)\right]\right\} \longleftrightarrow \cosh(mf)V(f)$$

and

$$-\frac{iW}{2\pi}\left\{\mathrm{sinc}\left[W\left(t+i\frac{m}{2\pi}\right)\right] - \mathrm{sinc}\left[W\left(t-i\frac{m}{2\pi}\right)\right]\right\} \longleftrightarrow \sinh(mf)V(f).$$

Therefore, we get

$$\mathrm{sinc}\left[W\left(t+i\frac{m}{2\pi}\right)\right] + \mathrm{sinc}\left[W\left(t-i\frac{m}{2\pi}\right)\right] = \frac{2Wt}{(Wt)^2 + (\frac{Wm}{2\pi})^2}\sin(Wt)\cosh\left(\frac{Wm}{2\pi}\right) + \frac{\frac{Wm}{\pi}}{(Wt)^2 + (\frac{Wm}{2\pi})^2}\cos(Wt)\sinh\left(\frac{Wm}{2\pi}\right). \tag{13}$$

Similarly

$$\begin{aligned}&\operatorname{sinc}\left[W\left(t+i\frac{m}{2\pi}\right)\right]-\operatorname{sinc}\left[W\left(t-i\frac{m}{2\pi}\right)\right]\\&=i\left[\frac{\frac{-Wm}{\pi}}{(Wt)^2+(\frac{Wm}{2\pi})^2}\sin(Wt)\cosh\left(\frac{Wm}{2\pi}\right)\right.\\&\quad\left.+\frac{2Wt}{(Wt)^2+(\frac{Wm}{2\pi})^2}\cos(Wt)\sinh\left(\frac{Wm}{2\pi}\right)\right].\end{aligned}\tag{14}$$

So the inverse Fourier transform of $X(f)$ leads to the following.

Case a): When $X(f)$ is even, then

$$\begin{aligned}x_e(t)=\frac{A_eW}{2\pi}&\left\{\operatorname{sinc}\left[W\left(t+\frac{m}{2\pi}\right)\right]\right.\\&\left.+\operatorname{sinc}\left[W\left(t-\frac{m}{2\pi}\right)\right]\right\}+\alpha\frac{A_eW}{2\pi}\left\{\operatorname{sinc}\right.\\&\left.\times\left[W\left(t+i\frac{m}{2\pi}\right)\right]+\operatorname{sinc}\left[W\left(t-i\frac{m}{2\pi}\right)\right]\right\}\end{aligned}$$

where A_e and α have the same definition as before, (9).

Substituting for (13), $x_e(t)$ is given by

$$\begin{aligned}x_e(t)=\frac{A_eW}{2\pi}&\left\{\operatorname{sinc}\left[W\left(t+\frac{m}{2\pi}\right)\right]\right.\\&\left.+\operatorname{sinc}\left[W\left(t-\frac{m}{2\pi}\right)\right]\right\}+\alpha\frac{A_eW}{2\pi}\\&\times\left\{\frac{2Wt}{(Wt)^2+(\frac{Wm}{2\pi})^2}\sin(Wt)\cosh\left(\frac{Wm}{2\pi}\right)\right.\\&\left.+\frac{\frac{Wm}{\pi}}{(Wt)^2+(\frac{Wm}{2\pi})^2}\cos(Wt)\sinh\left(\frac{Wm}{2\pi}\right)\right\}.\end{aligned}$$

This shows that $x_e(t)$ is a real signal in the time-domain.

Case b): When $X(f)$ is odd, then

$$\begin{aligned}x_o(t)=-\frac{iB_oW}{2\pi}&\left\{\operatorname{sinc}\left[W\left(t+\frac{m}{2\pi}\right)\right]\right.\\&\left.-\operatorname{sinc}\left[W\left(t-\frac{m}{2\pi}\right)\right]\right\}\\&-\beta\frac{iB_oW}{2\pi}\left\{\operatorname{sinc}\left[W\left(t+i\frac{m}{2\pi}\right)\right]\right.\\&\left.-\operatorname{sinc}\left[W\left(t-i\frac{m}{2\pi}\right)\right]\right\}\end{aligned}$$

where B_o and β are the same as before, (11).

Substituting for (14), $x_o(t)$ is given by

$$\begin{aligned}x_o(t)=-\frac{iB_oW}{2\pi}&\left\{\operatorname{sinc}\left[W\left(t+\frac{m}{2\pi}\right)\right]\right.\\&\left.-\operatorname{sinc}\left[W\left(t-\frac{m}{2\pi}\right)\right]\right\}+\beta\frac{B_oW}{2\pi}\\&\times\left\{\frac{\frac{-Wm}{\pi}}{(Wt)^2+(\frac{Wm}{2\pi})^2}\sin(Wt)\cosh\left(\frac{Wm}{2\pi}\right)\right.\\&\left.+\frac{2Wt}{(Wt)^2+(\frac{Wm}{2\pi})^2}\cos(Wt)\sinh\left(\frac{Wm}{2\pi}\right)\right\}.\end{aligned}$$

This shows that $x_o(t)$ is a complex signal in the time-domain.

D. Properties of the Solution Functions

In this section, we study the properties of the solution functions. The results are shown in the following theorems.

Theorem 1:

1) The sequence $\{m_j\}$, for $j=1,2,3,\ldots$, consists of the values which satisfy the even condition (10) and the even solution (9), and the sequence $\{m'_j\}$, for $j=1,2,3,\ldots$, consists of the values which satisfy the odd condition (12) and the odd solution (11). Both of these two sets of sequences are monotonically increasing and m_j and m'_j are interleaved with each other.
2) The union solution set $\{\psi_i(f)\}=\{X_{ej}(f)\cup X_{ok}(f)\}$, $i,j,k=1,2,3,\ldots,|f|\le W$, which consists of the even optimal functions (9) and the odd optimal functions (11), can be ordered as

$$\begin{aligned}&\sqrt{\frac{1}{(1+\alpha_1^2)W}}(\cos(m_1f)+\alpha_1\cosh(m_1f))\\&\sqrt{\frac{1}{(1-\beta_1^2)W}}(\sin(m'_1f)+\beta_1\sinh(m'_1f))\\&\sqrt{\frac{1}{(1+\alpha_2^2)W}}(\cos(m_2f)+\alpha_2\cosh(m_2f))\\&\sqrt{\frac{1}{(1-\beta_2^2)W}}(\sin(m'_2f)+\beta_2\sinh(m'_2f))\\&\quad\vdots\end{aligned}\tag{15}$$

Proof: See Appendix I. ■

Theorem 2: $\{\psi_i(f)\}$ is a complete, orthonormal basis in $L^2([-W,W])$.

Proof: See Appendix II. ■

V. Numerical Study

In this section, we make a numerical study to show the characteristics of the optimal solution functions $\{\psi_i(f)\}$. Before that, we first introduce the time-duration measure.

A. Time-Duration Measure

In this paper, we define two kinds of time-duration measures: the *minimum fourth-moment time-duration measure* on the whole real line, and the *time-duration energy concentration measure* in the time interval $[-T,T]$.

The minimum fourth-moment time-duration measure is defined as

$$\eta\triangleq\frac{\int_{-\infty}^{\infty}t^4|x(t)|^2dt}{\int_{-\infty}^{\infty}|x(t)|^2dt}=\frac{\lambda}{(2\pi)^4}\tag{16}$$

where λ is the eigenvalue defined by the fourth-order differential (7). The latter equality is obtained using the Parseval's Theorem as follows:

$$\begin{aligned}\int_{-\infty}^{\infty}t^4|x(t)|^2dt&=\langle t^4x,x\rangle\\&=\left\langle\frac{1}{(2\pi)^4}X^{(4)}(f),X(f)\right\rangle=\frac{\lambda}{(2\pi)^4}\langle x(t),x(t)\rangle.\end{aligned}$$

Here, we have used the (6) in the third equality.

TABLE I
PARAMETERS FOR THE EVEN FUNCTIONS FOR $W = 0.5$

Even Functions							
Index	mW	m	$\lambda = m^4$	α	$\eta = \frac{m^4}{(2\pi)^4}$	γ_e $(T = 5)$	γ_e (T=13)
1	2.365	4.7300	500.5467	0.1329	0.3212	0.3495	0.3693
2	5.4978	10.9956	$1.4618e+04$	-0.0058	9.3790	0.2288	0.2387
3	8.6394	17.2788	$8.9136e+04$	2.5031e-04	57.1919	0.1705	0.1806
4	11.781	23.5620	$3.0821e+05$	-1.0817e-05	197.7578	0.1080	0.1328
5	14.9226	29.8452	$7.9341e+05$	4.6744e-07	509.0712	0.0597	0.1157
6	18.0642	36.1284	$1.7037e+06$	-2.0200e-08	$1.0931e+03$	0.0312	0.1275
7	21.2057	42.4114	$3.2354e+06$	8.7292e-10	$2.0759e+03$	0.0192	0.1517
8	24.3473	48.6946	$5.6224e+06$	-3.7722e-11	$3.6075e+03$	0.0157	0.1679

TABLE II
PARAMETERS FOR THE ODD FUNCTIONS FOR $W = 0.5$

Odd Functions							
Index	$m'W$	m'	$\lambda' = (m')^4$	β	$\eta' = \frac{(m')^4}{(2\pi)^4}$	γ_o $(T = 5)$	γ_o (T=13)
1	3.9266	7.8532	$3.8035e+03$	0.0279	2.4404	0.0205	0.0332
2	7.0686	14.1372	$3.9944e+04$	-0.0012	25.6291	0.0564	0.0917
3	10.2102	20.4204	$1.7388e+05$	5.2035e-05	111.5674	0.0900	0.1487
4	13.3518	26.7036	$5.0849e+05$	-2.2486e-06	326.2570	0.1051	0.1803
5	16.4934	32.9868	$1.1840e+06$	9.7172e-08	759.6985	0.0956	0.1797
6	19.635	39.2700	$2.3782e+06$	-4.1992e-09	$1.5259e+03$	0.0680	0.1583
7	22.7765	45.5530	$4.3059e+06$	1.8146e-10	$2.7628e+03$	0.0358	0.1359
8	25.9181	51.8362	$7.2199e+06$	-7.8417e-12	$4.6325e+03$	0.0118	0.1270

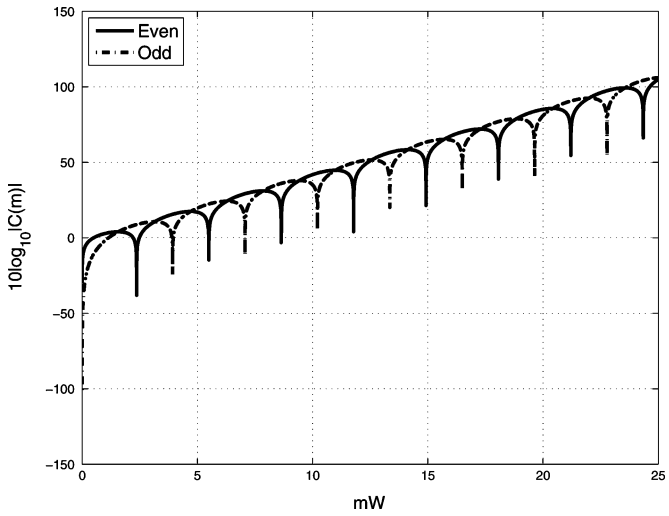

Fig. 1. Trend of the even condition function, $C_e(m)$ in (10), and odd condition function, $C_o(m)$ in (12), versus mW.

The time-duration energy concentration measure in the time interval $[-T, T]$ is defined as

$$\gamma \triangleq \frac{\int_{-T}^{T} |x(t)|^2 dt}{\int_{-\infty}^{\infty} |x(t)|^2 dt}. \tag{17}$$

B. Distribution of m and m'

In Fig. 1, the x axis denotes the values of mW and the y axis denotes the condition function. We take the y axis as $10 \log_{10} |C(m)|$. The label "even" means the even condition function, $C_e(m)$ in (10), and the label "odd" means the odd condition function, $C_o(m')$ in (12).

The downward peak points in the figure show the zero points of the condition functions, respectively. This figure shows: 1) the condition functions present the periodicity of $\cos x$ and $\sin x$; 2) the zero points mW and $m'W$ for the functions are interleaved each other, asserted in Theorem 1; and 3) the trend of the condition functions are increasing by the hyperbolic functions $\cosh x$ and $\sinh x$.

Table I and Table II list the first 8 values of m and m' when $W = 0.5$ for the even and odd condition functions in (10) and (12), respectively. These two Tables also include the value of α, β, eigenvalues $\lambda = m^4$ and $\lambda' = (m')^4$, time-duration measure η, (16), and time-duration energy concentration measure γ, (17), corresponding to each m and m' values. From these tables, we can see that for fixed W, the values of α and β decrease very quickly with increasing m and m'. For index $j \geq 3$

$$X_{ej}(f) \longrightarrow A_{ej} \cos(m_j f) \quad \text{and}$$
$$X_{oj}(f) \longrightarrow B_{oj} \sin(m'_j) f.$$

C. Characteristics of Basis Functions for Fixed $W = 0.5$

The characteristics of the basis functions with different values of m_j for the even function and $m_{k'}$ for the odd function with fixed bandwidth $W = 0.5$ are shown in Figs. 2 and 3.

Fig. 2 shows the even functions $X_e(f)$ and their corresponding inverse Fourier transform $x_e(t)$ vary with different value m_j in the frequency domain. From Fig. 2(a), we know that for the even function $X_e(f)$, except the end points, there is no zero point when $m = m_1, 2$ zero points when $m = m_2, 4$ zero points when $m = m_3$, and 6 zero points when $m = m_4$, etc. So we can establish that there are $2(j-1)$ zero points for the even function when $m = m_j$. The function $x_e(t)$ in Fig. 2(b) shows the waveform in the time-domain has sharper central portion, less main lobe and decays slowly when m_j decreases.

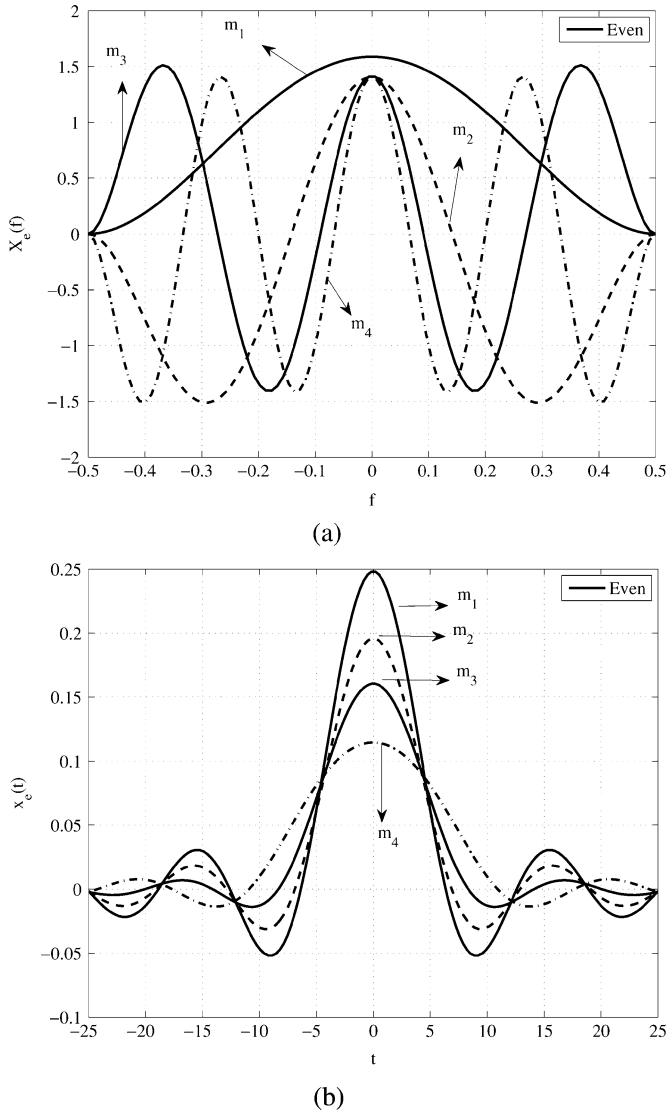

Fig. 2. The even function $X_e(f)$ and its inverse Fourier transform $x_e(t)$ versus variable m with $m = 1, 2, 3, 4$ for fixed $W = 0.5$. (a) $X_{em_j}(f)$ in the frequency domain. (b) $x_{em_j}(t)$ in the time-domain.

Fig. 3 depicts how the odd functions $X_o(f)$ and their inverse Fourier transforms $x_o(t)$ vary with different value m'_k in the frequency domain and in the time-domain. Fig. 3(a) indicates that for the odd function $X_{om'_k}(f)$, except the end points, there is 1 zero point when $m' = m'_1$, 3 zero points when $m' = m'_2$, 5 zero points when $m' = m'_3$ and 7 zero points when $m' = m'_4$. It is concluded that there are $2k - 1$ for the odd functions with $m' = m'_k$. Fig. 3(b) and (c) depict the real part and the imaginary part of the odd function $x_{om'_k}(t)$ versus the variable m' for fixed $W = 0.5$ in the time-domain. The magnitude of the real part is much smaller compared to the magnitude of the imaginary part. Therefore, as the value of m' increases, the odd signal approaches a pure complex signal as the real part approaches zero.

D. Minimum Fourth-Moment Time-Duration Measure and Energy Concentration Measure

Based on the definitions of the minimum fourth-moment time-duration measure (16) and the time-duration energy concentration measure (17), we have calculated these values and included them in the Tables I and II (for $W = 0.5$). Two cases for the time-duration energy concentration measure

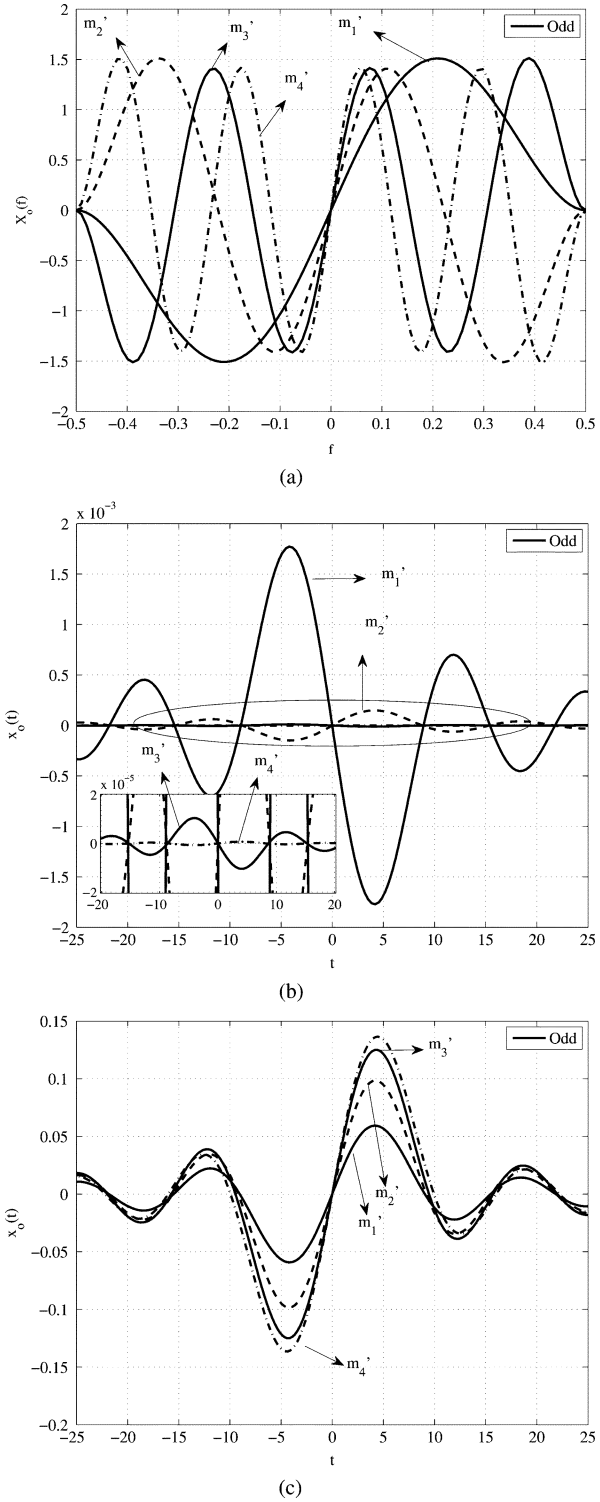

Fig. 3. The odd function $X_o(f)$ and its inverse Fourier transform $x_o(t)$ versus variable m' with $m' = 1, 2, 3, 4$ for fixed $W = 0.5$. (a) $X_{om'_k}(f)$ in the frequency domain. (b) The real part of $x_{om'_k}(t)$ in the time-domain, where the amplitude of Y-axis is 2×10^{-3}, the small panel is to show the real part of the waveform of $x_{om'_3}(t)$ and $x_{om'_4}(t)$ whose amplitudes are only 2×10^{-5}. (c) The imaginary part of $x_{om'_k}(t)$ in the time-domain, where the amplitude of Y axis is 0.1. Comparing to the real part in (b), the imaginary part in (c) dominates the whole waveform.

when $T = 5$ and $T = 13$ are considered. The tables indicate that: 1) the minimum fourth-moment time-duration measure η increases quickly; 2) the time-duration energy concentration measure γ_e decreases roughly as m increases; 3) γ_e increases as the measure interval T increases; and 4) $x_{e1}(t)$, the even function, has higher energy concentration measure than the other functions.

E. Comparison Between PSWF, Gabor and Our Basis Functions

Slepian's prolate spheroidal wave function (PSWF) is an optimal band-limited function bandwidth Ω which achieves the maximal energy in the time interval $[-T, T]$ [3]. PSWF satisfies the following eigenvalue equation

$$\int_{-\Omega/(2\pi)}^{\Omega/(2\pi)} \frac{\sin 2\pi T(f-f')}{\pi(f-f')}\psi(f')df' = \lambda\psi(f), \quad |f| \le \frac{\Omega}{2\pi}.$$

It is well known that no explicitly analytical formula for the PSWF exists. And only the discrete approximation of the PSWF by numerical computation is available [3], [23], [25].

Gabor's function is defined by [9]

$$\phi(f) = \frac{1}{\sqrt{W}} \sin\left(\frac{k\pi}{2W}f + \frac{k\pi}{2}\right), \quad |f| \le W$$

where $k \in \mathbf{Z}\backslash\{0\}$. The corresponding inverse Fourier transform is

$$\phi(t) = \frac{\sqrt{W}}{2\pi}\left\{\operatorname{sinc}\left[W\left(t + \frac{k}{4W}\right)\right] + \operatorname{sinc}\left[W\left(t - \frac{k}{4W}\right)\right]\right\}.$$

Take $k = 1$, we have

$$\phi_1(f) = \frac{1}{\sqrt{W}} \cos\left(\frac{\pi}{2W}f\right), \quad |f| \le W$$

and the corresponding inverse Fourier transform is

$$\phi_1(t) = \frac{\sqrt{W}}{2\pi}\left\{\operatorname{sinc}\left[W\left(t + \frac{1}{4W}\right)\right] + \operatorname{sinc}\left[W\left(t - \frac{1}{4W}\right)\right]\right\}.$$

Take the first basis functions of PSWF, Gabor and our basis functions as an example. Let the bandwidth $W = 0.5$ and the interested time-duration $T = 5$ for comparison. Then the time-bandwidth product for PSWF is $c = \Omega T = 2\pi WT = 15.7085$. Fig. 4 shows the first basis functions of Slepian PSWF, Gabor and our basis functions both in the frequency domain and in the time-domain. The energy for these three functions in $[-T, T]$ is 0.9999, 0.2806, and 0.3495 for PSWF, Gabor and our basis function. From this figure, we can see that: 1) Slepian's PSWF absolutely holds the best performance both in the time-domain due to its maximum energy concentration in the center; 2) our basis functions are a bit better than Gabor's function; and 3) our basis functions have larger main lobes.

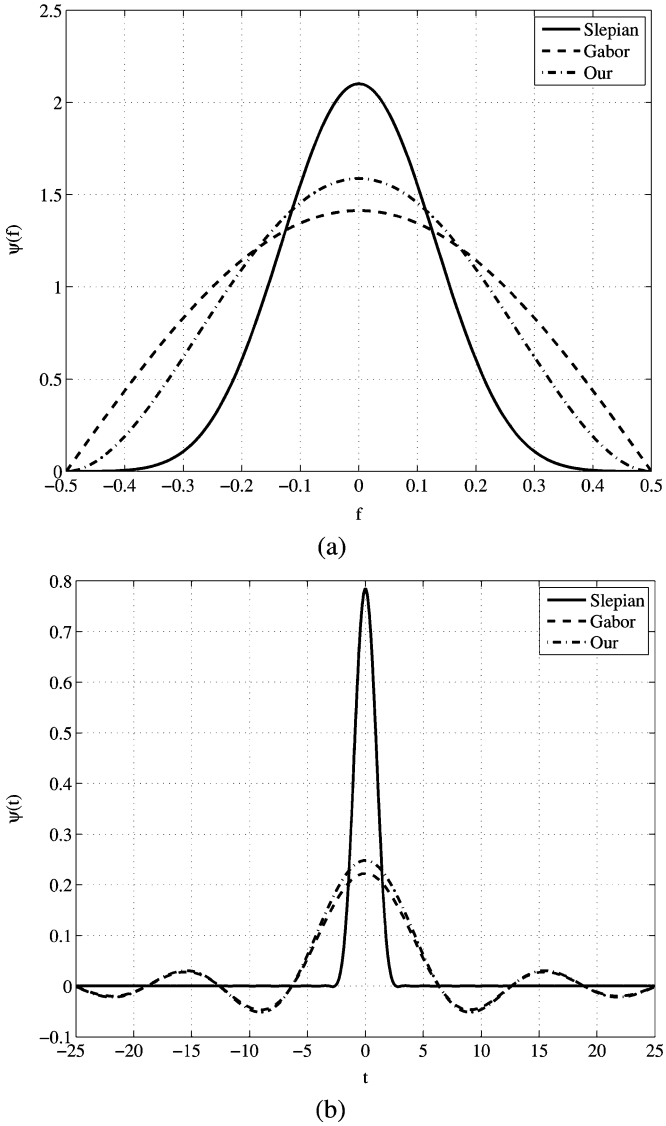

Fig. 4. Comparison of the first basis functions among the Slepian PSWF, Gabor and our basis functions when $W = 0.5$ and $T = 5$. (a) Comparison in the frequency domain. (b) Comparison in the time-domain.

VI. Applications

A. Optimal Waveforms for Communication Systems

The following study shows that the set of our optimal functions can be a better choice of waveform for some systems, such as radar system with higher range resolution requirement and data transmission with higher information rate, due to its fast decaying rate $O(1/t^3)$ which is faster than that of Slepian's PSWF $O(1/t)$ and Gabor's functions $O(1/t^2)$ and higher energy concentration in the main lobe. Therefore, our optimal functions are more powerful to counteract the intersymbol interference (ISI) and more robust for the signal detection.

We now compare our optimal functions with Gabor's function [9] which is optimal with respect to the minimum second-moment time-duration measure. Set $W = 0.5$. Our first even function $X_{e1}(f)$ with $m_1 = 4.7300$ is compared

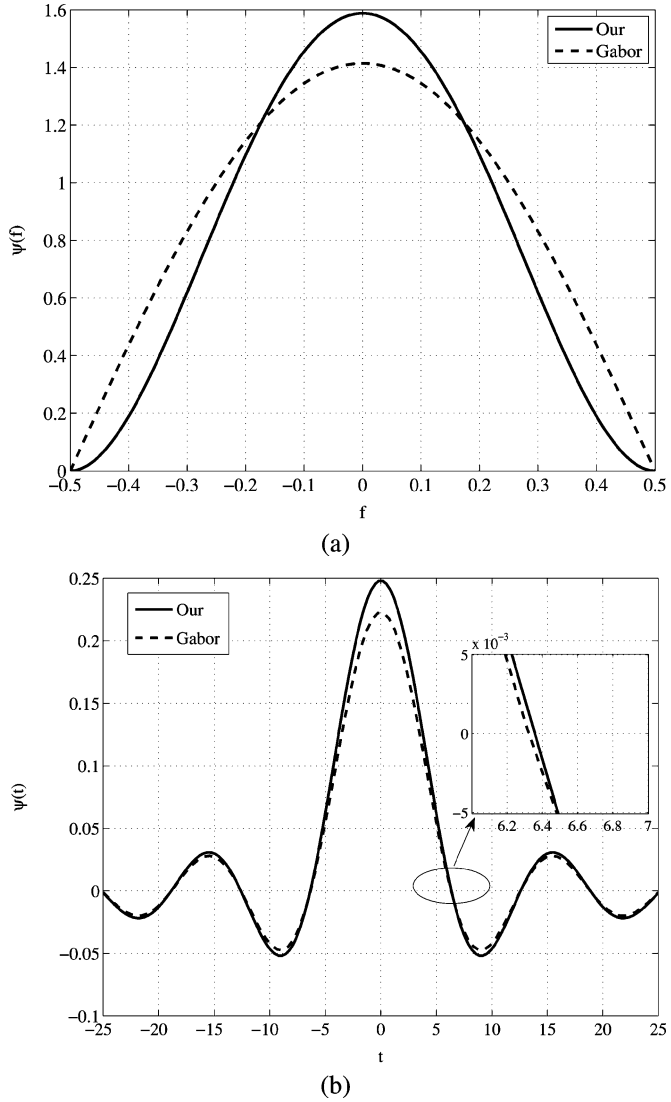

Fig. 5. Comparison of our optimal function $X_{e1}(f)$ with Gabor's function $\Phi_1(f)$ with $W = 0.5$. (a) Our optimal function $X_{e1}(f)$ and Gabor's function $\Phi_1(f)$ in the frequency domain. (b) Our optimal function $x_{e1}(t)$ and Gabor's function $\phi_1(t)$ in the time-domain. The small panel in (c) shows the main lobes of both functions, where the red (our optimal function) is a bit larger than the green one (Gabor's function).

with Gabor's function. Fig. 5 shows these functions both in the frequency domain and in the time domain. Obviously, comparing with Gabor's function, Fig. 5(b) indicates that our basis function: 1) has larger energy concentration in the center lobe; 2) higher peak value, comparing the 0.25 with 0.22; 3) and has quicker decaying rate. As Franks [28] showed that PSWF decays[1] like $1/t$ which is slower than Gabor's function acting like $1/t^2$, our optimal function holds the steepest decaying rate, a bit like $1/t^3$ [27]. The embedded small figure denotes that our function has a bit larger main lobe than that of Gabor.

Finally, we compare the time-duration concentration measure of our function with that of Gabor's function. The main lobe of the $x_{e1}(t)$ and $\phi_1(t)$ are $T_{x_{e1}} \approx 6.3536$ and $T_{\phi_1} \approx 6.3236$. By (17), the main lobe energy concentration is

$$\gamma_{x_{e1}} = \frac{\int_{-T_{x_{e1}}}^{T_{x_{e1}}} |x_{e1}(t)|^2 dt}{\int_{-\infty}^{\infty} |x(t)|^2 dt} = 0.3524,$$

$$\gamma_{\phi_1(t)} = \frac{\int_{-T_{\phi_1}}^{T_{\phi_1}} |\phi_1(t)|^2 dt}{\int_{-\infty}^{\infty} |x(t)|^2 dt} = 0.2828.$$

It shows our function has much higher main lobe energy concentration than Gabor's function's, though it has only a bit larger main lobe, which is a good alternative for radar system with higher resolution requirement.

B. Representation and Finite Dimensional Approximations

The eigenfunctions $\{\psi_i(f)\}$ form a complete, orthonormal basis in $L^2(-W, W)$, so we can use them to represent any band-limited function with maximal bandwidth W, extrapolate a band-limited function known only on the interval $(-T, T)$ and make an approximation in an interval to a band-limited function [3].

Suppose $S(f) \in L^2([-W, W])$ is a band-limited signal. Since $\{\psi_i(f)\}$ is an orthonormal basis in $L^2([-W, W])$, then we can represent

$$S(f) = \sum_{i=1}^{\infty} s_i \psi_i(f) \tag{18}$$

where

$$s_i = \int_{-W}^{W} S(f)\psi_i(f) df.$$

Based on the above Theorem 2 and the orthonormality of the basis functions, we can make a further detailed representation

$$S(f) = \sum_{j=1}^{\infty} a_j X_{ej}(f) + \sum_{k=1}^{\infty} b_k X_{ok}(f) \tag{19}$$

with

$$a_j = \int_{-W}^{W} S(f) X_{ej}(f) df \quad \text{and}$$

$$b_k = \int_{-W}^{W} S(f) X_{ok}(f) df.$$

Now we consider the dimensionality of the generic expansion (18) or (19) by a finite number of terms [30], [31]

$$S_N(f) = \sum_{i=1}^{N} s_i \psi_i(f)$$

with squared error

$$\delta_N = \|S(f) - S_N(f)\|^2 = \sum_{i=N+1}^{\infty} |s_i|^2.$$

Here, we take the square norm in $L^2([-W, W])$. It is well known that the dimensionality mainly depends on the basis functions $\{\psi_i(f)\}$, the explicit function $S(f)$ and the truncated error δ_N. As $\{\psi_i(f)\}$ is the optimum basis, it will achieve the

[1]We noted that although PSWFs decays like $1/t$, they are also uniformly small outside the interval of concentration and as a result the decay rate is irrelevant. The results obtained from the example in Fig. 4 confirms this observation.

best performance comparing with other basis functions. As our basis functions are complete, according to Fourier transform, we can also represent a signal in the time-domain

$$s_N(t) = \sum_{j=1}^{N} a_j x_{ej}(t) + \sum_{k=1}^{N} b_k x_{ok}(t).$$

Take the rectangle function (also called box function) as an example,

$$G(f) = \begin{cases} 1, & |f| < W; \\ 0, & |f| \geq W. \end{cases}$$

and

$$g(t) = \frac{W}{\pi} \operatorname{sinc}(Wt).$$

Since $G(f)$ is an even function in the frequency interval $[-W, W]$, according to the representation (19), we get

$$\begin{aligned} a_j &= \int_{-W}^{W} G(f) A_{ej}(\cos(m_j f) + \alpha_j \cosh(m_j f)) df \\ &= 2\int_{0}^{W} A_{ej}(\cos(m_j f) + \alpha_j \cosh(m_j f)) df \\ &= 2A_{ej}\left[\frac{\sin(m_j W)}{m_j} + \alpha_j \frac{\sinh(m_j W)}{m_j}\right] \\ &= \frac{4A_{ej}\sin(m_j W)}{m_j}. \end{aligned}$$

The last equality is obtained by substituting $\alpha_j = -\cos(m_j W)/\cosh(m_j W)$. We also have $b_k = 0$ for all k. Therefore

$$G(f) = \sum_{j=1}^{\infty} a_j X_{ej}(f),$$

$$G_N(f) = \sum_{j=1}^{N} a_j X_{ej}(f),$$

and the truncated squared error δ_N is

$$\delta_N = \|G(f) - G_N(f)\|^2 = \sum_{j=N+1}^{\infty} |a_j|^2.$$

Since $A_{ej} = 1/\sqrt{(1+\alpha_j^2)W}$ and $\alpha_j \longrightarrow 0$ as $j > 4$, we get

$$A_{ej} = 1/\sqrt{(1+\alpha_j^2)W} < 1/\sqrt{W}$$

and

$$|a_j| = \left|\frac{4A_{ej}\sin(m_j W)}{m_j}\right| \leq \left|\frac{4A_{ej}}{m_j}\right| < \frac{4}{\sqrt{W} m_j}$$

therefore, the truncated squared error is

$$\delta_N = \frac{16}{W}\sum_{j=N+1}^{\infty} \frac{\sin^2(m_j W)}{(1+\alpha_j^2)m_j^2} < \frac{16}{W}\sum_{j=N+1}^{\infty} \frac{1}{m_j^2}.$$

As we have shown in the above Theorem 2 and Subsection IV.D that the values of $m_j \longrightarrow \infty$ as $j \longrightarrow \infty$. So δ_N can be made as small as desired by making N sufficiently large. Similarly, we have

$$g_N(t) = \sum_{j=1}^{N} a_j x_{ej}(t).$$

Set $W = 0.5$. We depict the function $G_N(f)$ and $g_N(t)$ when $N = 8, 16, 50$ in Fig. 6. Obviously, when the number of items N increases, the approximation is better.

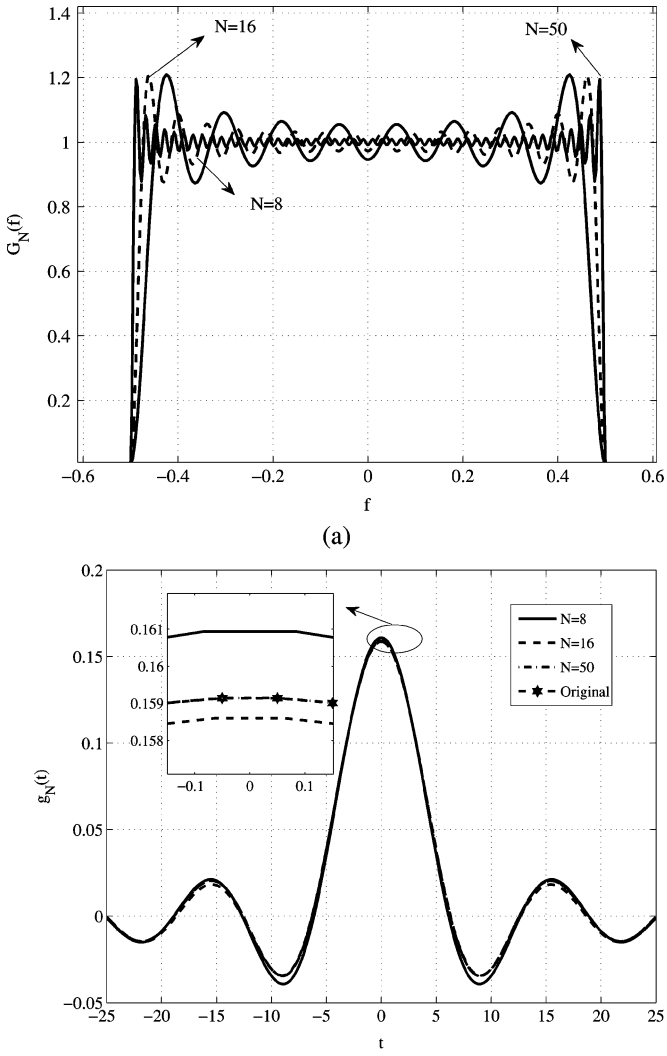

Fig. 6. Representation of a rectangle function with our optimal basis functions. N is the number of basis functions used, here $N = 8, 1650$. (a) Approximated function $G_N(f)$ in the frequency domain. (b) Approximated function $g_N(t)$ in the time-domain, the small panel in (b) is to show the difference around the peak value. When $N = 50, g_N(t)$ is approaching the original function.

VII. Conclusion

This paper uses the general constrained variational method of Franks to formulate the fourth-moment time-duration measure and determines a complete, orthonormal set of optimal band-limited functions. Comparing our optimal function with Gabor's function, the functions with higher moment weighting have better performances in the energy concentration in the main lobe and faster decaying side-lobes. This set of optimal

functions can be applied in communication and radar systems; and it can also be used to represent any band-limited signal with maximal bandwidth W and approximate a band-limited signal.

For higher-order moment time-domain weighting, t^k with $k > 4$, analogous results can be obtained based on our methods. It is also possible to treat the case of time-limited finite energy signals with frequency domain moment weighting, f^k, in an analogous way.

APPENDIX I
DISTRIBUTION OF m AND m' (THEOREM 1)

Proof: Let us consider the following three functions, first

$$f_1(x) = \tan(x), \quad f_2(x) = -\tanh(x) \text{ and } f_3(x) = \tanh(x).$$

As $0 \le \tanh(x) = \sinh(x)/\cosh(x) < 1$, for all $x \ge 0$, so the function $f_2(x)$ is a strictly monotonically increasing function with $f_2(\infty) \longrightarrow 1$; and $f_3(x)$ is a strictly monotonically decreasing function with $f_2(\infty) \longrightarrow -1$.

It is well known that: $\tan(x)$ is a periodical function with the period π, for any $k \in \mathbf{Z}$, $\tan(k\pi) = 0$, $\tan[(k\pi + \frac{\pi}{2})^-] \longrightarrow +\infty$ and $\tan[(k\pi + \frac{\pi}{2})^+] \longrightarrow -\infty$.

In a period, take $(k\pi - \pi/2, k\pi + \pi/2), k = 1, 2, 3, \ldots$ as an example, $\tan(x)$ monotonically increases from $-\infty$ to $+\infty$ as x increases from $k\pi - \pi/2$ to $k\pi + \pi/2$. So there must be a single crossing point x_{dk} with $-\tanh(x)$ in the lower half of the plane. And it also has a unique crossing point x_{uk} with $\tanh(x)$ in the upper half of the plane. And the values of $x_{dk} < x_{uk}$.

Now it is necessary to show that there has no crossing point for $\tan(x)$ and $\tanh(x)$ in the interval $[0, \pi/2)$. Take another function $g(x) = f_1(x) - f_3(x) = \tan(x) - \tanh(x)$, for $x \in [0, \pi/2)$. Let take the first derivative

$$\begin{aligned} g'(x) &= \frac{1}{\cos^2(x)} - \frac{1}{\cosh^2(x)} = \frac{\cosh^2(x) - \cos^2(x)}{\cosh^2(x)\cos^2(x)} \\ &= \frac{(\cosh(x) + \cos(x))(\cosh(x) - \cos(x))}{\cosh^2(x)\cos^2(x)} \\ &= \frac{\cosh(x) + \cos(x)}{\cosh^2(x)\cos^2(x)}(\cosh(x) - \cos(x)). \end{aligned}$$

As $\cosh(x) = (e^x + e^{-x})/2 \ge 1$ for any $x \ge 0$, and $0 < \cos(x) \le 1$ when $x \in [0, \pi/2)$, we can infer

$$g'(x) > 0.$$

So $g(x)$ is a strictly monotonically increasing function. And $g(0) = f_1(0) - f_3(0) = 0$, so in the interval $(0, \pi/2)$, $g(x) > 0$, i.e., $\tan(x) > \tanh(x)$, which means there is no crossing point between them.

It has been shown above that in $(0, \pi/2)$, $\tan(x) > 0$, $-\tanh(x) < 0$ and $\tanh(x) > 0$ and there is no crossing point for the functions $\tan(x)$ and $\tanh(x)$. So the first crossing point x_1 is the crossing point x_{d1} of $\tan(x)$ and $-\tanh(x)$; the second crossing point x_2 is the crossing point x_{u1} of $\tan(x)$ and $-\tanh(x)$; the third crossing point x_3 is the crossing point x_{d2} of $\tan(x)$ and $-\tanh(x)$; the fourth crossing point x_4 is the crossing point x_{u2} of $\tan(x)$ and $-\tanh(x)$; and so on.

Now relating to our proof of the theorem, let us check the condition functions. For fixed W, the even condition function is

$$\cos(mW)\sinh(mW) + \sin(mW)\cosh(mW) = 0$$

and the odd condition function is

$$\cos(mW)\sinh(mW) - \sin(mW)\cosh(mW) = 0.$$

So if $\cos(mW) \ne 0$, i.e., $mW \ne (k\pi + \pi/2), k \in \mathbf{Z}$, the even condition is changed into

$$\tan(mW) = -\tanh(mW)$$

and the odd condition is changed into

$$\tan(mW) = \tanh(mW).$$

From the above, the points $\{m_j W\}$ satisfying the even condition equation and the points $\{m'_k W\}$ satisfying the odd condition equation are interleaved, i.e., m_1, m'_1, m_2, m'_2, etc., and the values are monotonically increasing.

So the even solution functions $X_{ej}(f)$ and the odd solution functions $X_{ok}(f)$ can be ordered by the values of the value m_j and m'_k, i.e., as shown in (15). ■

APPENDIX II
PROOF OF THEOREM 2

Proof: From Section IV-B, we have an infinite set of complete optimal band-limited functions $\{\psi_i\} = \{X_{ej}(f) \cup X_{ok}(f)\}$, $i, j, k = 1, 2, 3, \ldots$ in the frequency interval $[-W, W]$ which consists of the even solution (9) and the odd solution (11). The completeness is from the fact that based on the boundary conditions and the initial conditions, we have got all possible functions satisfying the fourth-order (6) by the general solution (8). Now we want to show that this set is orthonormal. The orthonormality in the frequency interval $[-W, W]$ can be obtained from two methods: 1) by direct calculation of the orthonormality between any two functions; 2) by functional analysis with spectrum theorem for the compact self-adjoint operator: the corresponding eigenfunctions for distinct eigenvalues are orthogonal.

For the eigenvalue (7), D^4 is a differential operator which is unbounded and its inverse operator does not exist. Therefore, we define another operator

$$L = D^4 + I,$$

where I is the identity operator. So the eigenvalue equation is changed into

$$LX = (1 + \lambda)X.$$

Now we will show that the new operator L is self-adjoint and its inverse operator L^{-1} exists.

As we have discussed before that eigenvalue equation (7) has a real solution if and only if $\lambda \ge 0$. And when $\lambda = 0$, the solution is the zero function. Similarly, for the new eigenvalue (20), $LX = 0$ if and only if $X = 0$. So according to Theorem 4.5.2 in [32]: An operator L is invertible if and only if $Lu = 0$

implies $u = 0$. So L is invertible. Then its inverse operator L^{-1} exists.

Suppose $u, v \in \{\psi_i\}$, then

$$\langle Lu, v\rangle = \langle D^4u + u, v\rangle = \int_{L^2} v(D^4u)d\Omega + \int_{L^2} vud\Omega = \int_{L^2} (u''v'' + uv)d\Omega,$$

and

$$\langle v, Lu\rangle = \langle v, D^4u + u\rangle = \int_{L^2} v(D^4u)d\Omega + \int_{L^2} vud\Omega = \int_{L^2} (u''v'' + uv)d\Omega = \langle Lu, v\rangle.$$

So L is a self-adjoint operator.

Therefore, according to inverse differential operator Theorem 5.10.2 [32], L^{-1} is a self-adjoint compact operator from $L^2(-W, W)$. According to the Spectral theorem of self-adjoint compact operator, L^{-1} has a complete set of orthonormal eigenfunctions and its eigenvalues are real. Based on the Theorem 5.10.5 [32], L and L^{-1} have the same eigenfunctions and have the reciprocal eigenvalues. So L has an complete set of orthonormal eigenfunctions. As we also know that for distinct eigenvalues, their corresponding eigenfunctions are orthogonal.

From the Theorem 1, we have known that the values of m_j and m'_k are different. So the eigenvalues of L equaling to m^4 are different, too. Therefore, the eigenfunctions are orthogonal. As $X_e(f)$ and $X_o(f)$ are band-limited, unit energy signals, i.e., they are orthonormal. ■

ACKNOWLEDGMENT

The authors would like to thank Dr. B. Andrews, a senior lecture in the Mathematical Science Institute, Australian National University, who gave us help in the proof of the completeness of our basis functions.

REFERENCES

[1] Q. Jin, Z. Q. Luo, and K. M. Wong, "An optimum complete orthonormal basis for signal analysis and design," *IEEE Trans. Inf. Theory*, vol. 40, no. 3, pp. 732–742, May 1994.

[2] G. Lachs, "Optimization of signal waveforms," *IEEE Trans. Inf. Theory*, vol. IT-9, pp. 95–97, Apr. 1963.

[3] D. Slepian and H. O. Pollak, "Prolate spheroidal wave functions, Fourier analysis and uncertainty—I," *Bell Syst. Tech. J*, vol. 40, pp. 43–63, Jan. 1961.

[4] H. J. Landau and H. O. Pollack, "Prolate spheroidal wave functions, Fourier analysis and uncertainty-II," *Bell Syst. Tech. J.*, vol. 40, no. 1, pp. 65–84, Jan. 1961.

[5] A. Papoulis, "Minimum-bias windows for high-resolution spectral estimates," *IEEE Trans. Inf. Theory*, vol. IT-19, no. 1, pp. 9–12, Jan. 1973.

[6] D. Slepian, "On bandwidth," *Proc. IEEE*, vol. 64, no. 3, pp. 292–300, Mar. 1976.

[7] A. Nuttall and F. Amoroso, "Minimum Gabor bandwidth of M orthogonal signals," *IEEE Trans. Inf. Theory*, vol. 14, no. 5, pp. 440–444, July 1965.

[8] A. Nuttall, "Minimum rms bandwidth of M time-limited signals with specified code or correlation matrix," *IEEE Trans. Inf. Theory*, vol. IT-14, no. 5, pp. 699–707, Sep. 1968.

[9] D. Gabor, "Theory of communication," *J. Inst. Elec. Eng.*, vol. 93, no. 26, pt. III, pp. 429–457, Nov. 1946.

[10] L. C. Potter and K. S. Arun, "Energy concentration in band-limited extrapolation," *IEEE Trans. Acoust., Speech, Signal Process.*, vol. 37, no. 7, pp. 1027–1041, Jul. 1989.

[11] R. A. Kennedy, W. Zhang, and T. D. Abhayapala, "Spherical harmonic analysis and model-limited extrapolation on the sphere: Integral equation formulation," in *Proc. Int. Conf. Signal Process. Commun. Syst., ICSPCS'2008*, Gold Coast, Australia, Dec. 2008, p. 6.

[12] A. Wyner and H. Landau, "Optimum waveform signal sets with amplitude and energy constraints," *IEEE Trans. Inf. Theory*, vol. IT-30, no. 4, pp. 615–622, Jul. 1984.

[13] X. Liang, B. ChuanXing, C. XinZhao, and C. Jian, "Resolution enhancement of nearfield acoustic holography by interpolation using band-limited signal restoration method," *Chinese Sci. Bull.*, vol. 53, no. 20, pp. 3142–3150, Oct. 2008.

[14] D. Slepian, "Prolate spheroidal wave functions, Fourier analysis, and uncertainty V- the discrete case," *Bell Syst. Tech. J.*, vol. 57, no. 5, pp. 1371–1430, May–Jun. 1978.

[15] A. Papoulis and M. Bertran, "Digital filtering and prolate functions," *IEEE Trans. Circuit Theory*, vol. CT-19, no. 6, pp. 674–681, Nov. 1972.

[16] Y. Xu, S. Haykin, and R. J. Racine, "Multiple window time-frequency distribution and coherence of EEG using Slepian sequences and Hermite functions," *IEEE Trans. Biomed. Eng.*, vol. 67, no. 7, pp. 861–866, Jul. 1999.

[17] G. A. Prieto, R. L. Parker, D. J. Thomson, F. L. Vernon, and R. L. Graham, "Reducing the bias of multitaper spectrum estimates," *Geophys. J. Int.*, vol. 171, pp. 1269–1281, 2007.

[18] P. P. Mitra and H. Maniar, "Concentration maximization and local basis expansions (LBEX) for linear inverse problems," *IEEE Trans. Biomed. Eng.*, vol. 53, no. 9, pp. 1775–1782, Sep. 2006.

[19] G. G. Walter and X. Shen, "Sampling with prolate spheroidal wave functions," *Sampling Theory in Signal and Image Process.*, vol. 2, no. 1, pp. 25–52, Jan. 2003.

[20] G. G. Walter and X. Shen, "Wavelet based on prolate spheroidal wave functions," *J. Fourier Anal. Appl.*, vol. 10, no. 1, pp. 1–26, 2004.

[21] G. G. Walter and X. Shen, "Peroidic prolate spheroidal wavelets," *J. Funct. Anal. Optimiz.*, vol. 26, no. 7–8, pp. 953–976, 2005.

[22] X. Shen and G. G. Walter, "Construction of periodic prolate spheroidal wavelets using interpolation," *Numer. Funct. Anal. Optimiz.*, vol. 28, no. 3–4, pp. 445–466, 2007.

[23] C. J. Bouwkamp, "On spheroidal wave functions of order zero," *J. Math. Phys.*, vol. 26, pp. 79–92, 1947.

[24] F. A. Grunbaum, "Eigenvectors of a Toeplitz matrix: Discrete version of the prolate spheroidal wave functions," *SIAM J. Alg. Disc. Meth.*, vol. 2, no. 2, pp. 136–141, Jun. 1981.

[25] H. Xiao, V. Rokhlin, and N. Yarvin, "Prolate spheroidal wavefunctions, quadrature and interpolation," *Inverse Problems*, vol. 17, no. 4, pp. 805–838, 2001.

[26] G. Beylkin and L. Monzon, "On generalized Gaussian quadratures for exponentials and their applications," *Appl. Comp. Harm. Anal.*, vol. 12, no. 3, pp. 332–373, 2002.

[27] E. A. Fain and M. K. Varanasi, "Minimum bandwidth basis functions for the fourth-moment bandwidth measure," in *Proc. IEEE Int. Symp. Inf. Theory*, Sorrento, Italy, Jun. 2000, p. 416.

[28] L. E. Franks, *Signal Theory*. Englewood Cliffs, NJ: Prentice-Hall, 1969.

[29] L. Wei, R. A. Kennedy, and T. A. Lamahewa, "Band-limited signal concentration in time-frequency," in *Proc. Int. Conf. Signal Process. Commun. Syst. ICSPCS'2009*, Omaha, NE, Sep. 28–30, 2009, pp. 6–0.

[30] H. J. Landau and H. O. Pollak, "Prolate spheroidal wave functions, Fourier analysis and uncertainty—III: The dimension of the space of essentially time- and band-limited signals," *Bell Syst. Tech. J*, vol. 41, pp. 1295–1336, July 1962.

[31] R. A. Kennedy and T. D. Abhayapala, "Spatial concentration of wavefields: Towards spatial information content in arbitrary multipath scattering," in *Proc. 4th Austral. Commun. Theory Workshop, AusCTW-2003*, Melbourne, Australia, Feb. 2003, pp. 38–45.

[32] L. Debnath and P. Mikusinski, *Introduction to Hilbert Spaces With Applications*. San Diego, CA: Academic, 1990.

Liying Wei (S'09) received the B.E. degree from Xidian University, the M.E. degree from Beijing University of Posts and Telecommunications, China, in 2002 and 2006, respectively.

She is currently a Ph.D. student with the Research School of Information Science and Engineering, Australian National University. Her current research interest includes spatial signal processing, spectral analysis, *ad hoc* networks and sensor networks, wireless communications, and optical fiber communications.

Rodney A. Kennedy (S'86–M'88–SM'01–F'05) received the B.E. degree from the University of New South Wales, Sydney, Australia, the M.E. degree from the University of Newcastle, and the Ph.D. degree from the Australian National University, Canberra.

He was with the Commonwealth Scientific and Industrial Research Organization (CSIRO) on the Australia Telescope Project for three years. He is currently a professor and was the Head of the Department of Information Engineering, Research School of Information Sciences and Engineering, Australian National University. His research interests are in the fields of digital signal processing, spatial information systems, digital and wireless communications, and acoustical signal processing. More recently, his research has included more life science related to medical image processing and biological ion channel modeling.

Tharaka A. Lamahewa (M'06) received the B.E. degree from the University of Adelaide, South Australia, in 2000, and the Ph.D. degree from the Australian National University in 2007.

He was with Motorola Electronics Pvt Ltd., Singapore, for two years as a software design engineer. From 2006 to 2007, he was an algorithm design engineer with Nanoradio AB, Melbourne, Australia. He is now with the Applied Signal Processing Group, Research School of Information Sciences and Engineering, Australian National University. He also holds a position with National ICT Australia (NICTA) as a wireless researcher. His research interests include information theory of time-varying fading channels, cooperative diversity, space-time coding and space-time-frequency channel modeling, body-area networks, underwater communications, and signal processing on the unit sphere.